Reducing the Phase Error for Finite-Difference Methods Without Increasing the Order

John W. Nehrbass, Jovan O. Jevtić, and Robert Lee, *Member, IEEE*

***Abstract*—The phase error in finite-difference (FD) methods is related to the spatial resolution and thus limits the maximum grid size for a desired accuracy. Greater accuracy is typically achieved by defining finer resolutions or implementing higher order methods. Both these techniques require more memory and longer computation times. In this paper, new modified methods are presented which are optimized to problems of electromagnetics. Simple methods are presented that reduce numerical phase error without additional processing time or memory requirements. Furthermore, these methods are applied to both the Helmholtz equation in the frequency domain and the finite-difference time-domain (FDTD) method. Both analytical and numerical results are presented to demonstrate the accuracy of these new methods.**

***Index Terms*—Finite-difference methods.**

I. Introduction

THERE exists a rich history of finite-difference (FD) techniques that have been applied to the disciplines of mathematics and science. In essence, FD is a technique that replaces derivatives in a governing set of differential equations with difference approximations obtained by sampling functions at discrete locations. The first electromagnetic (EM) FD method was introduced to the electromagnetics community in 1966 by Yee [1] and was implemented in the time domain. Since this first introduction, the FD method has greatly matured and gained wide acceptance. While many of the present electromagnetic (EM) FD techniques are adapted from methods in other disciplines, this paper shows that these traditional methods can be greatly improved if they are optimized specifically for electromagnetic models.

When one uses computational methods to study electromagnetic wave problems, the two major sources of error are boundary errors and numerical dispersion errors. Boundary errors are generated when changes in material properties occur or when an artificial termination is placed at the outer boundary of the problem domain. Even when boundaries contribute only a small fraction of the total problem, the contributing effects can be significant. Over the past 30 years, a considerable amount of effort has been devoted to reducing the error at the outer boundary [2]–[8]; however, there has been very little effort made to reduce the error caused by material boundaries for electromagnetic problems.

Numerical dispersion error in finite methods has received considerable attention [9], [10]. This numerical dispersion error causes a phase error as the wave propagates through the grid. The propagating wave accumulates phase error at every grid point. Thus, this type of error can become a limiting factor for electrically large structures of geometries contain high Q cavities. Typically, one reduces the numerical dispersion error by either choosing a finer grid or a higher order FD scheme. However, both finer grids and higher order schemes imply larger memory requirements and greater computation time. Relatively little effort has been devoted to the reduction of these errors by less costly and more innovative ways [11]–[14]. In this paper, we present a systematic approach to modify traditional FD methods (in both the time and frequency domains) to minimize the numerical dispersion error without increasing the computation costs. Furthermore, we consider simple methods to reduce errors which occur at material interfaces.

In the FD approximation of Maxwell's equations, the numerical wave number is dependent on the grid spacing and the physical wave number. In addition, the numerical wave number is anisotropic, i.e., it is dependent on the direction the wave propagates through the grid. When examining the central difference approximation (Cartesian coordinates) of the Helmholtz equation, a numerical dispersion analysis for a propagating plane wave reveals that the numerical wave number is always greater than the physical wave number for all angles of propagation. This paper demonstrates that by appropriately modifying the traditional central difference coefficients of the Helmholtz equation approximation, the effects of numerical dispersion can be greatly reduced. In fact, the coefficients are chosen such that the average phase error, over all angles of propagation, is zero. This concept is also extended to the finite-difference time-domain (FDTD) method. To obtain a zero average phase error at a specified frequency, the wave velocity is changed such that the average numerical wave number (over all propagation angles) is equal to the physical wave number. With a judicious choice of frequency for the optimization, we can obtain an improvement over a large bandwidth. The beauty of this concept is that current FD codes based on the traditional FD methods can be modified by only changing one or two lines in the computer codes. Thus, the vast wealth of FDTD tools developed over the past 30 years can be significantly improved with only trivial modifications.

The remainder of this paper is organized as follows. The next section presents optimal FD equations for the Helmholtz equation in one, two, and three dimensions. The one-dimensional (1-D) case is presented to demonstrate the concepts which motivated this paper. The major derivation

Manuscript received January 23, 1997; revised December 29, 1997.

The authors are with the ElectroScience Laboratory, Department of Electrical Engineering, The Ohio State University, Columbus, OH 43212 USA.

Publisher Item Identifier S 0018-926X(98)06102-X.

is done for the two-dimensional (2-D) case. The derivation for the three-dimensional (3-D) case is straightforward; only the final 3-D equations are presented. In addition to reducing the phase error, we present a scheme for matching the FD equations at 2-D material boundaries. These ideas are also extended to the FDTD method. Finally, numerical verifications are presented along with some conclusions.

II. Optimal Finite-Difference Equations for the Helmholtz Equation

A. The 1-D Helmholtz Equation

Consider the 1-D Helmholtz equation applied to a homogeneous medium in the absence of boundaries, given by

$$\frac{d^2f(x)}{dx^2} + k^2 f(x) = 0 \tag{1}$$

where k is the wave number. Traditionally, the finite difference approximation of the above equation is achieved by replacing the second-order derivative with the central difference approximation which is given as

$$f''(x) = \frac{f(x+h) - 2f(x) + f(x-h)}{h^2}. \tag{2}$$

Substituting (2) into (1) produces the FD approximation of the Helmholtz equation given as

$$\left(\frac{d^2f(x)}{dx^2} + k^2 f(x)\right)\Big|_{x=0} = \frac{f_1 + f_2 - (2 - k^2h^2)f_0}{h^2} + O(h^2) \tag{3}$$

where f_0, f_1, and f_2 are the values of $f(x)$ sampled at the locations as shown in Fig. 1. Notice that this provides a second-order accurate solution. Further, if $f(x)$ represents a Taylor series expansion of an arbitrary function, the above provides the most accurate approximation of the Helmholtz equation while sampling $f(x)$ at only three discrete locations. This approximation however does suffer from numerical dispersion errors. If one now uses *a priori* information by assuming $f(x)$ to be equal to the general solution of the 1-D Helmholtz equation, given as

$$f(x) = Ae^{jkx} + Be^{-jkx} \tag{4}$$

a more accurate approximation can be obtained. Instead of using the central difference approximation for the second-order derivative, let us approximate $f''(x)$ as

$$f''(x) \approx \frac{f(x+h) - wf(x) + f(x-h)}{h^2} = \frac{2\cos(kh) - w}{h^2} f(x) \tag{5}$$

where the coefficient w is to be optimized. The analytical solution of $f''(x)$ is

$$f''(x) = -k^2 f(x). \tag{6}$$

Therefore, we observe that for this case, an optimal value of w is $w = 2\cos(kh) + k^2h^2$ and not $w = 2$ as was used in the central difference approximation. The new FD approximation of the Helmholtz equation can now be approximated as

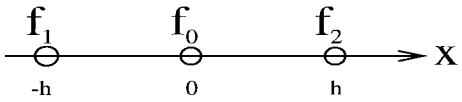

Fig. 1. A three-point stencil for a 1-D problem using a regular grid.

$$\frac{f_1 + f_2 - (w - k^2h^2)f_0}{h^2} = \frac{2\cos kh - (w - k^2h^2)}{h^2}(A + B) \tag{7}$$

and is identically satisfied when $w = k^2h^2 + 2\cos(kh)$. Note that by merely changing the normalized center node differencing coefficient from 2to $2\cos(kh) + k^2h^2$, the new approximation becomes numerically dispersionless.

Comparing the two center node differencing coefficients

$$\text{Standard FD center coefficient } (w)2 \tag{8}$$

$$\text{Corrected FD center coefficient } (w)2\cos(kh) + k^2h^2 = 2 + O(h^4) \tag{9}$$

one notices that they differ only in the fourth-order term. The corrected FD method achieves a more accurate solution than the conventional method by reducing the numerical dispersion effects; therefore, in the rest of this paper, we will refer to this new method as the reduced dispersion (RD) FD method in the frequency domain and RD FDTD in the time domain.

Motivated by the above analysis, we seek to develop a FD approximation for the Helmholtz equation which has better accuracy than the standard central difference approximation for wave problems in 2-D and 3-D. In achieving these goals, it is desirable to keep the same number of sampling nodes with the same formulation, change only the center stencil FD coefficient, reduce the discretization and numerical dispersion error, and maintain second order accuracy. The next two sections present solutions for the optimal coefficients required in the 2-D and 3-D FD approximations of the Helmholtz equation.

B. The 2-D Helmholtz Equation

In this section, a 2-D wave problem for a homogeneous medium in the absence of boundaries is considered. This problem is modeled by the 2-D Helmholtz equation and is given as

$$\frac{\partial^2 f(x,y)}{\partial x^2} + \frac{\partial^2 f(x,y)}{\partial y^2} + k^2 f(x,y) = 0 \tag{10}$$

where again, k is the wave number. For this problem it is helpful to consider the standard five-point stencil in 2-D as illustrated in Fig. 2. We can study numerical dispersion effects by launching a plane wave into the computation domain and predicting how well the numerical method models the plane wave. Using the standard central difference approximation ($w = 2$) for both second order derivatives ($\partial^2/\partial x^2$ and $\partial^2/\partial y^2$) and exciting the region by the plane wave

$$f(x,y) = e^{jk(x\cos\theta + y\sin\theta)} \tag{11}$$

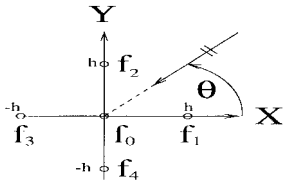

Fig. 2. A five-point stencil for a 2-D problem using a regular grid.

yields the relationship

$$\frac{\partial^2 f(x,y)}{\partial x^2}+\frac{\partial^2 f(x,y)}{\partial y^2}+k^2 f(x,y)|_{x=0}^{y=0} = \frac{f_1+f_2+f_3+f_4-(4-k^2h^2)f_0}{h^2}+\text{Res} \quad (12)$$

where f_0, f_1, f_2, f_3, and f_4 are the values of the plane wave sampled at the locations as defined in Fig. 2. The 2-D case produces a second-order accurate residual term given as

$$\text{Res}(\theta)=\frac{2\cos(kh\cos\theta)+2\cos(kh\sin\theta)-(4-k^2h^2)}{h^2} \quad (13)$$

which can be expanded as

$$\text{Res}(\theta)=O(h^2)=R_0+R_1\cos(4\theta)+R_2\cos(8*\theta)+\cdots. \quad (14)$$

The application of (12) implies that the condition

$$f_1+f_2+f_3+f_4-(4-k^2h^2)f_0=0 \quad (15)$$

must be ideally satisfied for some numerical plane wave

$$\hat{f}(x,y)=\hat{A}e^{j\hat{k}(x\cos\theta+y\sin\theta)}. \quad (16)$$

The percent error in magnitude of the numerical plane wave without boundary conditions is very small. A more significant factor is the difference in phase between the numerically calculated wave and the analytical wave. In this paper, the phase error in degrees per wave length is defined as

$$\text{Phase}\,(f(\lambda))-\text{Phase}(\hat{f}(\lambda))=360*(1-\hat{k}/k). \quad (17)$$

Notice that the residual term, and thus the phase error per wavelength, is now anisotropic with respect to how the wave propagates through the grid.

Like the 1-D case, we seek to reduce the phase error by using the modified CD equation and optimizing w. Notice that we only modify the central node (f_0) weight, as allowing the weights on the other nodes $(f_1 f_2 f_3 f_4)$ to be dissimilar would imply a biased direction of propagation. Since the 2-D phase error is now anisotropic, no choice of w will completely remove its effect. One can however remove the isotropic part of the residual (R_0) by a proper choice of w, which is equivalent to minimizing the average phase error over all possible angles. To find w, we must solve

$$\int_0^{2\pi} 2\left[\cos(kh\cos\theta)+\cos(kh\sin\theta)-(w-k^2h^2/2)\right]d\theta = 0. \quad (18)$$

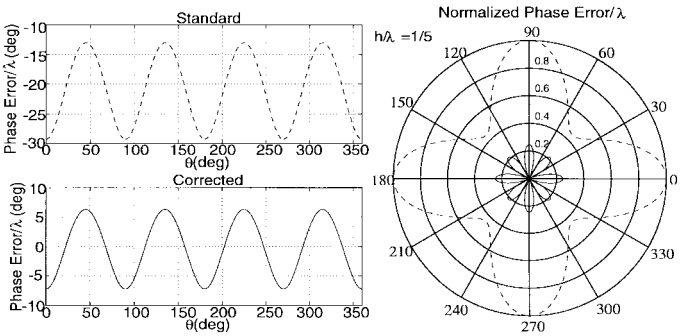

Fig. 3. Standard and corrected phase error for a plane wave versus θ.

Solving for w in the above, one can compare the two center node coefficients for the 2-D case

$$\text{Standard FD center coefficient } (w)4 \quad (19)$$

$$\text{Corrected FD center coefficient } (w)\,4J_0(kh)+k^2h^2 = 4+O(h^4) \quad (20)$$

where $J_0(x)$ is the zeroth-order Bessel function of the first kind. Once again, they differ in only the fourth-order term. Notice that the residual term associated with the RD FD method (Res')

$$\text{Res}'(\theta)=O(h^2)=R_1\cos(4\theta)+R_2\cos(8\theta)+\cdots \quad (21)$$

has no isotropic component (R_0'). Fig. 3 graphically illustrates the improvement. Notice that in addition to reducing the phase error for all angles of incidence, we have introduced twice as many zero crossings. In other words, the phase error will become minimized twice as often in the corrected case as for the standard case. Furthermore, the phase error has now both a positive and negative component, thus allowing the possibility of error cancellation instead of an absolute cumulative error.

C. The 3-D Helmholtz Equation

The 3-D wave problem for a homogeneous medium in the absence of boundaries is considered by using the 3-D Helmholtz equation, given as

$$\nabla^2 f(x,y,z)+k^2 f(x,y,z)=0 \quad (22)$$

where k is the wave number. Applying the modified second-order accurate CD approximation to the Laplacian operator yields the FD approximation

$$\begin{aligned}\nabla_h^2 f(x,y,z)=&[f(x+h,y,z)+f(x-h,y,z)\\&+f(x,y+h,z)+f(x,y-h,z)\\&+f(x+h,y,z+h)+f(x,y,z-h)\\&-wf(x,y,z)]\frac{1}{h^2}.\end{aligned} \quad (23)$$

Since a plane wave traveling at an any arbitrary angle (θ, ϕ) exactly solves (22), the error associated with the FD approximation can be minimized by selecting a w such that the average error over all angles (θ, ϕ) for a plane wave is zero. When comparing the traditional central difference coefficient to the optimal coefficient for a 3-D plane wave that propagates

in an unbiased direction, we again notice changes in the fourth order:

$$\text{Standard central difference coefficient } (w)6 \tag{24}$$

$$\text{Corrected coefficient } (w)6j_0(kh) + k^2h^2 = 6 + O(h^4). \tag{25}$$

j_0 is the zeroth-order spherical Bessel function of the first kind. Notice that for all three dimensions, the new optimized coefficient used in approximating the second-order derivative converges to the conventional coefficient as $kh \to 0$. Thus the numerical solution converges to the exact solution with second-order accuracy $O(h^2)$:

$$\text{New CD weight} \qquad \text{Conventional CD weight} \tag{26}$$

$$\begin{aligned}
&\text{3D case } w = (kh)^2 + 6j_0(kh) \lim_{kh\to 0} w = 6\\
&\text{2D case } w = (kh)^2 + 4J_0(kh) \lim_{kh\to 0} w = 4\\
&\text{1D case } w = (kh)^2 + 2\cos(kh) \lim_{kh\to 0} w = 2.
\end{aligned} \tag{27}$$

III. Material Interfaces

In conventional methods, modeling the boundary between two dissimilar materials presents particular difficulties. When a sampling node lies on the boundary between two different materials one must decide what value to use for the constituent parameters at the discontinuity. Typically, a weighted value of the two materials is used, however this weighting reduces second-order accurate methods to locally first-order accurate methods. This has the same effect as introducing artificial reflections or placing an artificial source at the material discontinuity. Since any error generated locally transmits through and reflects from the discontinuous material boundaries, it contaminates the entire solution.

In the RD FD method the boundaries are handled in a special way that reduces the significance of these boundary generated errors. Consider the 2-D boundary value problem of Fig. 4 in which two different materials (ϵ_A, μ_A, and ϵ_B, μ_B) are present. The concept of virtual nodes is used to handle the discontinuity. The material is first virtually extended so that it "appears" homogeneous as looking from each dielectric material. Modeling each material separately yields the equations

$$0 = [A_1 + A_2 + A_3 + A_4 - 4J_0(k_A h)A_0] \tag{28}$$

$$0 = [B_1 + B_2 + B_3 + B_4 - 4J_0(k_B h)B_0] \tag{29}$$

where $k_A = \omega\sqrt{\mu_A\epsilon_A}$ and $k_B = \omega\sqrt{\mu_B\epsilon_B}$ are the wave numbers of the respective materials and A_i, B_i, and f_i are the function values sampled at the locations as depicted in Fig. 4. Notice that these two equations are both second-order accurate, however there are now ten nodes used to model the problem when five were originally used. By enforcing continuity of the tangential electric and magnetic field values, one can derive a single governing difference equation requiring five node values. In the TM case (E_z, H_x, and H_y), we apply continuity of E_z directly and continuity of the tangential magnetic field through a proper specification on the normal derivative of E_z,

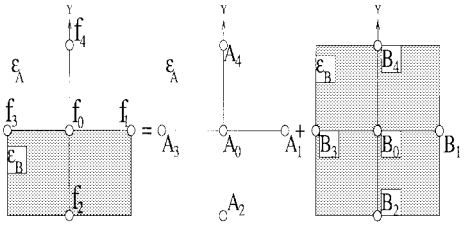

Fig. 4. Edge boundary value problem.

whereas for the TE case (H_z, E_x, and E_y), we apply continuity of H_z directly and continuity of the tangential electric field through a proper specification on the normal derivative of H_z. Thus, continuity of either E_z or H_z implies that $A_1 = B_1$, $A_0 = B_0$, and $A_3 = B_3$.

A second-order accurate difference equation is needed to solve for the normal derivative at the boundary. The analytical solution for the derivative of a plane wave is given as

$$\frac{\partial}{\partial y} e^{j(\vec{K}\cdot\vec{R})} = jk_y e^{j(\vec{K}\cdot\vec{R})} \tag{30}$$

while the general numerical FD approximation may be found as

$$aA_2 + bA_0 + dA_4 = \left(ae^{-jk_y h} + b + de^{jk_y h}\right)e^{j(\vec{K}\cdot\vec{R})}. \tag{31}$$

The numerical solution matches the analytical solution "closest" when $a = -d$ and $b = 0$ which gives a residual $R(\theta)$ relation of

$$R(\theta) = k_y - 2dj\,\sin(k_y h). \tag{32}$$

Since $k_y = k\sin(\theta)$ is a function of angle, and in general a wave may propagate in any direction without preference, the optimal value of d is calculated by minimizing the residual as

$$\int_0^{2\pi} R(\theta)\,\sin\theta d\theta. \tag{33}$$

The $\sin(\theta)$ weight is chosen since the analytical solution has a $\sin(\theta)$ variation. Solving (33) gives a value of

$$d_i = \frac{k_i}{4J_1(k_i h)} \tag{34}$$

where $J_1(x)$ is a first-order Bessel function of the first kind. Using the above and enforcing the continuity of normal directives, we obtain

$$\begin{aligned}
&\text{TE case } \mu_B d_A(A_4 - A_2) = \mu_A d_B(B_4 - B_2)\\
&\text{TM case } \epsilon_B d_A(A_4 - A_2) = \epsilon_A d_B(B_4 - B_2).
\end{aligned} \tag{35}$$

Combining all of the above yields the desired difference equation as

$$\begin{aligned}
0 = {} & (w_A + w_B)(f_1 + f_3) + 2w_B f_2 + 2w_A f_4\\
& - 4(w_B J_0(k_B h) + w_A J_0(k_A h))f_0
\end{aligned} \tag{36}$$

$$\begin{aligned}
&\text{TE case } w_i = \frac{hk_i}{4J_1(k_i h)\mu_i}\\
&\text{TM case } w_i = \frac{hk_i}{4J_1(k_i h)\epsilon_i}.
\end{aligned} \tag{37}$$

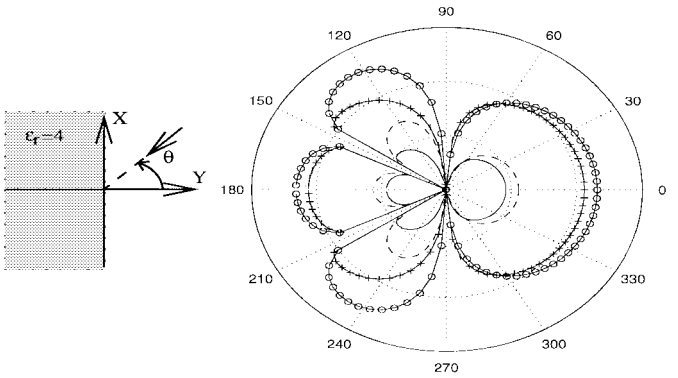

Fig. 5. Boundary error for optimal and standard coefficients.

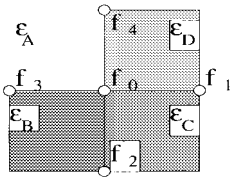

Fig. 6. Solution for a corner value problem.

The final solution preserves the physical relations but becomes first-order accurate. This accuracy is greatly improved compared to the conventional method. Since it has already been shown that the coefficients for (28) and (29) are optimal, we will illustrate the difference obtained for dielectric interfaces when using the coefficients of (37) versus the traditional value of two. Fig. 5 shows the error obtained for both polarizations when a plane wave is incident at a dielectric boundary at some angle θ. The error is defined as the absolute value of the difference between the complex reference solution and the complex calculated solution. As we will see in Section V, this error may be the dominant one in the solution.

This idea is extended to corner boundary value problems. Fig. 6 illustrates a corner where four different dielectrics combine. By enforcing continuous tangential fields between adjacent materials, the following difference equation is formed:

$$\begin{aligned}0 =&(w_A+w_B)f_3+(w_B+w_C)f_2+(w_C+w_D)f_1\\&+(w_D+w_A)f_4-2[w_AJ_0(k_Ah)+w_BJ_0(k_Bh)\\&+w_CJ_0(k_Ch)+w_DJ_0(k_Dh)]f_0.\end{aligned}\tag{38}$$

The extension to 3-D can be similarly derived.

IV. Optimal FDTD Coefficients

In this section we use the FDTD method to approximate our solution. The first part of this study concentrates on optimizing the FDTD coefficients at a single frequency. The effects of these changes over a band of frequencies is then discussed. Consider a 2-D TM polarized steady state plane wave propagating in free space in the absence of boundary conditions. The analytical solution, assuming an $\exp(j\omega t)$ time variation, is

$$\vec{E}=(\hat{y}\cos\theta-\hat{x}\sin\theta)e^{-jk(x\cos(\theta)+y\sin(\theta))}e^{j\omega t}\tag{39}$$

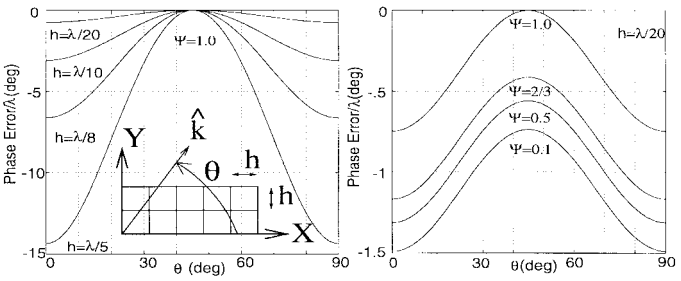

Fig. 7. Phase error for different grid resolutions.

where ω is the angular frequency of the wave. For a uniform mesh and a plane wave traveling at an angle θ with respect to the grid (see Fig. 7) the numerical solution is

$$\vec{E}=(\hat{y}\cos\theta-\hat{x}\sin\theta)e^{-j\hat{k}(x\cos(\theta)+y\sin(\theta))}e^{j\omega n\Delta t}\tag{40}$$

where the 2-D wave numbers k and $\hat{k}$ are related by the FDTD transcendental dispersion equation [15]

$$\frac{h^2}{\Delta t^2v^2}\sin^2\left(\frac{\omega\Delta t}{2}\right)=\sin^2\left(\frac{h}{2}\hat{k}\cos\theta\right)+\sin^2\left(\frac{h}{2}\hat{k}\sin\theta\right)\tag{41}$$

where

Δt	discrete time step size;
$v=1/\sqrt{\mu\epsilon}$	velocity of the wave;
$\hat{k}$	numerical wave number.

In order to guarantee numerical stability, the Courant stability condition requires

$$\Delta t\le\frac{h}{v\sqrt{N_D}}\tag{42}$$

where N_D is the spatial dimension. For 2-D ($N_D=2$) the quantity Ψ is defined as

$$\Psi=\frac{v\Delta t}{h}\sqrt{2}\tag{43}$$

with the condition $0<\Psi\le 1$ satisfying numerical stability requirements. Using the above, the dispersion relationship in 2-D is rewritten as

$$\begin{aligned}\frac{2}{\psi^2}\sin^2\left(\frac{h}{\omega\Delta t}2\right)=&\sin^2\left(\frac{h}{\lambda}\frac{\hat{k}}{k}\pi\cos\theta\right)\\&+\sin^2\left(\frac{h}{\lambda}\frac{\hat{k}}{k}\pi\sin\theta\right).\end{aligned}\tag{44}$$

The phase error, which is $\pi/2$ periodic, is illustrated in Fig. 7 for various spatial resolutions. When solving the transcendental equation (44) for $\hat{k}$ at a given angle $\theta\in[0,\pi/2]$ one may observe that the best results are always obtained at $\theta=\pi/4$, while the worst results are obtained at $\theta=0$ and $\pi/2$.

The dispersion equation is exactly solved ($\hat{k}=k$) when $\theta=\pi/4$ and $\Psi=1$. At all other angles θ and values of Ψ, the numerical value of $\hat{k}$ exceeds the physical value. The effect of lowering ψ causes the phase error curve to shift even farther from zero. Since $\hat{k}/k\ge 1$ for all θ, it is desirable to lower the numerical wave number such that the average value over all

θ is equal to the physical wave number (k). Ideally, we want to shift the phase error curve to have a zero average value.

Observe that we can reduce the $\hat{k}(\theta)$ relation by replacing the numerical value used to approximate v with a slightly larger numerically compensated propagation velocity v_c as

$$v_c = v_r v. \tag{45}$$

The optimal value of v_c is chosen such that the new dispersion curve $\hat{k}_c(\theta)$ is equal to k in the average sense, i.e.,

$$k = \frac{1}{2\pi} \int_0^{2\pi} \hat{k}_c(\theta)\, d\theta. \tag{46}$$

Note that by increasing v to v_c, the dispersion curve is not only shifted, but its shape becomes slightly more isotropic. It can be shown that for a grid spacing of $(h/\lambda < 1/5)$, v_r can be found in closed form as

$$v_r = \left. \frac{\sqrt{2}\sin\left(\dfrac{\pi\psi h}{\sqrt{2}\lambda}\right)}{\psi\sqrt{\sin^2\left(\dfrac{h}{\lambda}\pi\cos\theta\right) + \sin^2\left(\dfrac{h}{\lambda}\pi\sin\theta\right)}} \right|_{\theta=\pi/8}. \tag{47}$$

Similarly, a closed form solution for the 3-D case can be found as shown in (48) at the bottom of the page. Although the above relations are derived at only a single frequency, the phase error is reduced over a wide bandwidth.

V. Numerical Verifications

A. Helmholtz Scattering Example

This section is intended to provide further support for the previously derived statements. The first example we consider is a dielectric cylinder ($\epsilon_r = 4$) in the shape of a cavity (Fig. 8). The cylinder is excited by a TE-polarized plane wave traveling to the right with the incident field H_z^i having a magnitude of one. First-order absorbing boundary conditions are placed along the truncation boundaries. The magnetic field H_z is calculated and compared to a reference solution, which is obtained with a fine spatial resolution of 40 nodes per freespace wavelength. The results are then recalculated by three different methods. For each of these methods, the spatial resolution is reduced to only 20 nodes per freespace wavelength. In the first method, we use the central difference weights as applied to the Helmholtz equation. In the second method the corrected RD weights are used at all the nodes with no special treatment done at the dielectric interfaces (material properties at the interface are averaged). In the third method, we continue to use the corrected weights when we are not considering the nodes at the dielectric interfaces; however, for the interface, we use the special FD equation developed in Section III.

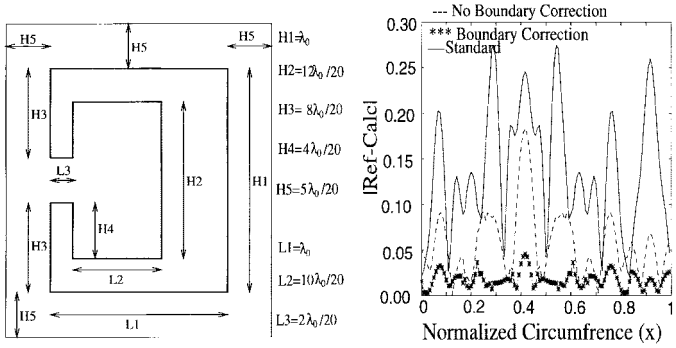

Fig. 8. Errors observed along the scatterer's boundary.

Fig. 8 illustrates the error generated when calculating the results for these three cases. The error is defined as the absolute value of the difference between calculated and reference field values. In the figure, the error is plotted versus the normalized circumference around the boundary of the scatterer. Starting at the lower right corner of the scatterer $(x = 0)$, and proceeding clockwise around circumference of the scatterer, the results are identified and the errors calculated.

The value of the solution on the surface of this dielectric structure is between zero and two; therefore, it is clear that there is significant error when the standard FD method is used. From the figure, it is also apparent that the solution is only somewhat improved when the homogeneous Helmholtz difference equation is corrected and vastly improved when the boundary finite difference equations are also corrected. In the next section we illustrate how these concepts can be applied to the time-domain formulations.

B. FDTD Corrected Examples

In this section the effects of correcting the FDTD equations are demonstrated. Two different examples are chosen to help support the concepts presented thus far. In the first example, a parallel plate wave guide filled with free space (see Fig. 9) is used. A TE_1 modulated Gaussian pulse is launched at the opening of the wave guide where the field values are calculated at the center of the waveguide, 5 cm from the opening. For this problem the cell size is chosen to be $\lambda/h = 12$ at 6 GHz. Both the standard FDTD method and the RD FDTD method are for 6 GHz. The phase errors per wavelength in the solution for these two method are illustrated in Fig. 9. At the design frequency of 6 GHz, the corrected method shows over a three times reduction in phase error. At lower frequencies, we notice that the new method does better than the standard method up to a certain frequency. At this frequency and lower

$$v_r = \left. \frac{\sqrt{3}\sin\left(\dfrac{\pi\psi h}{\sqrt{3}\lambda}\right)}{\psi\sqrt{\sin^2\left(\dfrac{h}{\lambda}\pi\cos\theta\right) + \sin^2\left(\dfrac{h}{\lambda}\pi\sin\theta\cos\phi\right) + \sin^2\left(\dfrac{h}{\lambda}\pi\sin\theta\sin\phi\right)}} \right|_{\theta=\pi/8}^{\phi=4\pi/27} \tag{48}$$

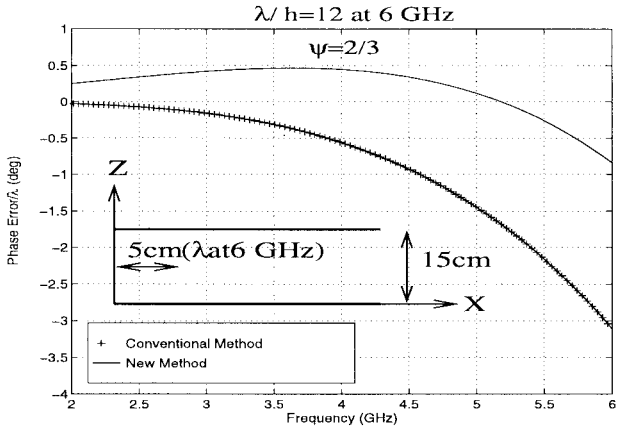

Fig. 9. A comparison of the phase error per wavelength generated when calculating for the fields inside a parallel plate waveguide.

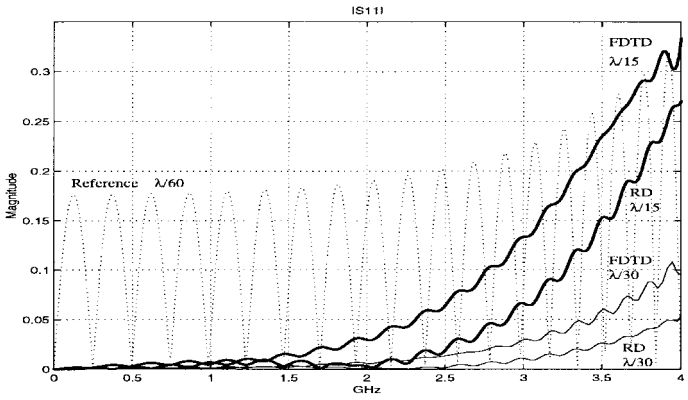

Fig. 10. Reflection coefficient S_{11} for a dielectric block placed in a parallel plate waveguide. The dashed line represents the reference solution. The solid lines represent the absolute value of the difference between the computed solution and the reference solution.

in the spectrum, for these angles of propagation, the standard method does better. However, the phase error of the corrected method never exceeds the maximum phase error generated at the design frequency. Also, recall that at lower frequencies, waves travel shorter distances with respect to the wavelength and therefore errors at lower frequencies are not expected to be as significant.

The geometry chosen for the second example is shown in Fig. 11. Since phase error accumulates as the wave propagates, the improvement can be better appreciated for electrically large structures. For this example, a simple dielectric block is placed symmetrically inside the center of a 5-cm-wide parallel plate waveguide filled with free space and the reflection S_{11} and transmission S_{21} coefficients are calculated. The relative dielectric constant of the block is chosen as $\epsilon_r = 4$. The length and width of the block is fixed at 50 and 2 cm, respectively, which is equivalent to 6.7 and 0.27 free-space wavelengths at 4 GHz. A ten-cell-thick parabolic conductive profile PML absorber is placed at each end port in order to truncate the problem domain. Without the dielectric block present, reflections from the PML absorber are observed to be at least 80 dB below the incident wave. A reference solution for this problem is calculated with a spatial resolution of $\lambda/h = 60$ at 4 GHz. The structure is illuminated by a

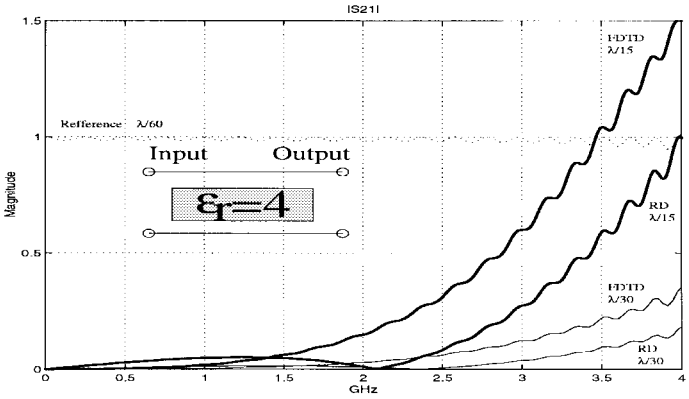

Fig. 11. Transmission coefficient S_{21} for a dielectric block placed in a parallel plate waveguide. The dashed line represents the reference solution. The solid lines represent the absolute value of the difference between the computed solution and the reference solution.

Gaussian pulse whose parameters are chosen such that there is significant spectral content from dc to 4 GHz. The excitation is assumed to be a TEM wave. As the pulse hits the dielectric block, energy is scattered in all directions and the reflected and transmitted waves are no longer TEM. We next recompute the reflection and transmission coefficients S_{11} and S_{21} using spatial resolutions of $\lambda/15$ and $\lambda/30$ at 4 GHz for both the FDTD method and the RD FDTD method. We can obtain a good approximation of the error by taking the absolute value of the difference of each method with the reference solution over a frequency range from dc to 4 GHz as shown in Fig. 11.

As expected, the RD FDTD method gives better results than the FDTD method for both spatial resolutions near the design frequency of 4 GHz. The RD FDTD method also gives better results at lower frequencies down to at least 2 GHz. Below 2 GHz the two methods vary in which method produces less error; however, notice that the magnitude of the errors at the lower frequencies are much smaller and thus less significant. Also observe that the improvement is better for the transmission coefficient than for the reflection coefficient due to the fact that we evaluate S_{21} at a location farther from the excitation than S_{11}, thus giving the wave more distance to accumulate phase error.

VI. Computational Savings

One can view the effect of the reduced dispersion scheme in two ways. The first is to compare the accuracy that one obtains with the improved method over the original method when both are applied to the same grid. The second way is to determine the computational savings that one obtains with the new method relative to the old for a given accuracy. The first approach is presented in the previous section. The second approach is presented in this section.

Let us consider the finite difference frequency domain method. For the 2-D case, the RD FD method with a grid spacing of $\lambda/8$ produces the same average phase error as the standard FD method with a grid spacing of $\lambda/20$. The memory savings is approximately a factor of 6.25. The speedup in computation time is dependent on the matrix method used. For a direct sparse solver, the computational complexity for

2-D problems is $N^{1.5}$ where N is the number of unknowns, while for an iterative solver such as the conjugate gradient method, the computational complexity is NM where M is the number of iterations needed for the solution to converge. In general M is dependent on N. For the direct and iterative solver, we expect the RD FD method to be 16 and $6.25P$ times faster, respectively, than the conventional FD method, where P is the ratio of the number of iterations of the new method over the number of iterations for the conventional FD method.

For the 3-D case, the RD FD method with a grid spacing of $\lambda/11$ produces the same average phase error as the conventional FD method with a grid spacing of $\lambda/20$. The memory savings is approximately a factor of 6. For the 3-D case the computational complexity of the iterative method remains the same; however, the computational complexity of the direct solver is now N^2. Thus, the computational speedup of the RD FD method relative to the conventional FD method is 36 for the direct sparse solver and $6P$ for the iterative solver.

A similar analysis is carried out for the FDTD method at $\Psi = 0.5$ and at the frequency for which the reduced dispersion optimization is done. For the 2-D case, the RD FDTD method with a grid spacing of $\lambda/9$ produces the same average phase error as the conventional FDTD method with a grid spacing of $\lambda/20$. The memory and computational savings are a factor of 9 and 11, respectively. For the 3-D case, the RD FDTD method with a grid spacing of $\lambda/12$ produces the same average phase error as the conventional FDTD method with a grid spacing of $\lambda/20$. The memory and computational savings are a factor of 4.6 and 7.7, respectively.

VII. Summary

In this paper, we present an alternative way of obtaining a FD equations for the wave equation in both the frequency and time domain. The new FD equations are based on an optimization of the FD coefficient for plane waves propagating through the grid. The resulting solutions have less phase error than the standard FD methods. Thus, with the new method one can use a coarser grid than the standard FD methods while maintaining the same accuracy. Because the new FD method contains less phase error, we refer to it as a reduced dispersion or RD FD method. The RD FD method has been demonstrated both in the frequency and time domain. The results shown in this paper demonstrate the computational savings that one can achieve relative to the standard FD methods. Because of its simplicity, it can be easily implemented into current FD codes without much effort.

References

[1] K. S. Yee, "Numerical solution of initial boundary value problems involving Maxwell's equations in isotropic media," *IEEE Trans. Antennas Propagat.*, vol. AP-14, pp. 302–307, Apr. 1966.

[2] B. Enquist and A. Majda, "Radiation boundary conditions for the numerical simulation of waves," *Math Comp.*, vol. 31, pp. 629–651, 1977.

[3] K. K. Mei and J. Fang, "Superabsorption: A method to improve absorbing boundary conditions," *IEEE Trans. Antennas Propagat.*, vol. 40, pp. 1001–1010, Sept. 1992.

[4] R. Higdon, "Absorbing boundary conditions for difference approximations to the multidimensional wave equation," *Math Comp.*, vol. 47, pp. 437–459, Oct. 1986.

[5] Z. P. Liao, H. L. Wong, B. P. Yang, and Y. F. Yuan, "A transmitting boundary for transient wave analysis," *Scientia Sinica (Ser. A)*, vol. 27, pp. 1063–1073, Oct. 1984.

[6] J. Berenger, "A perfectly matched layer for the absorption of electromagnetic waves," *Computational Phys.*, vol. 114, pp. 185–200, Oct. 1994.

[7] W. C. Chew and W. H. Weedon, "A 3-D perfectly matched medium from modified Maxwell's equation with stretched coordinates," *Microwave Opt. Technol. Lett.*, vol. 7, pp. 599–604, Sept. 1994.

[8] Z. S. Sacks, D. M. Kingsland, R. Lee, and J. F. Lee, "A perfectly matched anisotropic absorber for use as an absorbing boundary condition," *IEEE Trans. Antennas Propagat.*, vol. 43, pp. 1460–1463, Dec. 1995.

[9] R. Lee and A. C. Cangellaris, "A study of discretization error in the finite element approximation of wave solutions," *IEEE Trans. Antennas Propagat.*, vol. 40, pp. 542–549, May 1992.

[10] A. C. Cangellaris and R. Lee, "On the accuracy of numerical wave simulations based on finite methods," *J. Electromagn. Waves Applicat.*, vol. 6, no. 12, pp. 1635–1653, 1992.

[11] A. Taflove, *Computational Electrodynamics the Finite-Difference Time-Domain Method.* Norwood, MA: Artech House, 1995.

[12] J. B. Cole, "A high accuracy FDTD algorithm to solve microwave propagation and scattering problems on a coarse grid," *IEEE Trans. Microwave Theory Tech.*, vol. 43, pp. 2053–2058, Sept. 1995.

[13] ———, "A nearly exact second-order finite-difference time-domain wave propagation algorithm on a coarse grid," *Comput. Phys.*, vol. 8, no. 6, pp. 730–734, 1994.

[14] M. F. Hadi, M. Piket-May, and E. T. Thiele, "A modified FDTD (2,4) scheme for modeling electrically large structures with high phase accuracy," in *12th Annu. Rev. Progress Appl. Comput. Electromagn.*, Monterey, CA, Mar. 1996, vol. 2, pp. 1023–1030.

[15] K. S. Kunz and R. J. Luebbers, *The Finite Difference Time Domain Method for Electromagnetics.* Boca Raton, FL: CRC, 1993.

John W. Nehrbass was born in Buffalo, NY, in 1967. He received the B.S. (electrical engineering) and M.S. degree (electromagnetics) from Arizona State University, Tempe, in 1989 and 1991, respectively, and the Ph.D. degree (electrical engineering) from The Ohio State University, Columbus, in 1996.

He has been with the Aeronautical System Center (ASC) Major Shared Resource Center (MSRC) at Wright-Patterson Air Force Base, OH, as part of the Department of Defenses (DoD) High-Performance Computing Modernization Program since September 1996. He is employed through the Ohio Supercomputer Center and has been helping the DoD integrate electromagnetic algorithms to massively parallel platforms.

Jovan O. Jevtić, for a biography, see the August 1994 issue of this Transactions.

Robert Lee (S'82–M'83) received the B.S.E.E. degree in 1983 from Lehigh University, Bethlehem, PA, and the M.S.E.E. and Ph.D. degrees from the University of Arizona, Tucson, in 1988 and 1990, respectively.

From 1983 to 1984, he worked for Microwave Semiconductor Corporation, Somerset, NJ, as a Microwave Engineer. From 1984 to 1986 he was a Member of the Technical Staff at Hughes Aircraft Company, Tucson, AZ. From 1986 to 1990 he was a Research Assistant at the University of Arizona. In addition, from 1987 through 1989 (summers) he worked at Sandia National Laboratories, Albuquerque, NM. Since 1990 he has been at The Ohio State University, Columbus, where he is currently an Associate Professor. His major research interests are in the analysis and development of finite methods for electromagnetics.

Dr. Lee is a member of the International Union of Radio Science (URSI) and was a recipient of the URSI Young Scientist Award in 1996.